GANESH COLLEGE OF ENGINEERING

(Approved by AICTE, New Delhi & Affiliated to Anna University, Chennai)

Attur Main Road, Mettupatti, Salem - 636 111, Tamilnadu, India

Phone: 0427 - 2211212, +91 9865440414

E-Mail: principal@ganeshenggcollege.org   www.ganeshenggcollege.org

Learn. Rise. Excel

3.2.1 Number of papers published per teacher in the Journals notified on UGC website during the year

Title of paper	Name of the author/s	Department of the teacher	Name of journal	Year of publication	ISSN number	Link to the recognition in UGC enlistment of the Journal
Effect of EDM parameters on material removal rate, tool wear rate and geometrical errors of aluminium material	Dr.N.Senthil kumar	Mechanical	sciencedirect	2023	2214-7853	https://www.sciencedirect.com/science/article/abs/pii/S2214785320318289
Effects of process parameter on performance measures in electrical discharge machining using copper and brass electrodes	Dr.N.Senthil kumar	Mechanical	sciencedirect	2023	2214-7853	https://www.sciencedirect.com/science/article/abs/pii/S2214785320306611
Investigations and optimization of EDM parameters of conductive ceramic composites: a review	Dr.N.Senthil kumar	Mechanical	AIS	2023	2195-4356	https://link.springer.com/chapter/10.1007/978-981-19-7150-1_16
Investigation of welding speed on tensile strength of MIG welded Hastelloy C-276 joints	Dr.N.Senthil kumar	Mechanical	AIS	2023	020006 (2022)	https://link.springer.com/chapter/10.1007/978-981-19-7150-1_16
Design and Finite Element Analysis of a Concentric Tube Heat Exchanger	S. Sivakumar	Mechanical	IJIRT	2024	SSN: 2349-6002	https://ijirt.org/Article?manuscript=164229

PRINCIPAL

PRINCIPAL

Ganesh College of Engineering
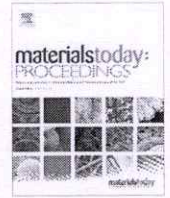
Attur Main Road, Mettupatti,

SALEM-636 111

Effect of EDM parameters on material removal rate, tool wear rate and geometrical errors of aluminium material

L. Selvarajan [a,*], R. Sasikumar [b], N. Senthil Kumar [a], Prabu Kolochi [c], P. Naveen Kumar [d]

[a] Department of Mechanical Engineering, Mahendra Institute of Technology, Namakkal, India
[b] Department of Mechanical Engineering, Mahendra Engineering College (Autonomous), Namakkal, India
[c] Master's in Applied Mechanics, Ecole Centrale Nantes, France
[d] Department of Mechanical Engineering, Mahendra Institute of Engineering and Technology, Namakkal, India

ARTICLE INFO

ABSTRACT

This investigation reveals the paradigm of EDM in this experiment to expel the metal from Al7075 with a performed Copper electrode. Aluminium7075 has the most elevated quality, higher firmness, and diminished thickness. Aluminium7075 is utilized prevalently in exceedingly focused on applications, for example, brackets, milk churns, mineral skips, cranes, external tank and scaffolds. Though EDM offers simple machinability joined with an excellent surface finish. Machine parameters of foremost noteworthiness, such as current (amp), pulse off time, pulse on time (μ sec), fluid pressure (kg/cm^2) and spark gap (mm) are contemplated utilizing Taguchi L_{18} orthogonal array. With the help of mean effective plots, tool wear rate (TWR), metal removal rate (MRR), cylindricity, circularity, and perpendicularity are examined. Information on such output levels and their impact on performance was investigated. The aftereffect of the investigation, the metal removal rate (MRR) increases when the current (10 amp) and pulse on time (29 μs) is increased. The tool wear rate (TWR) improves when the current (10 amp) and pulse on time (27 μs) is improved at the same time spark gap (0.4 mm) is reduced. And finally, the geometrical tolerance is also improved.
© 2019 Elsevier Ltd.
Selection and Peer-review under responsibility of the scientific committee of the International Mechanical Engineering Congress 2019: Materials Science.

1. Introduction

Due to the mechanized and sophisticated forms of the instrument electrode, the electric discharge machining (EDM) has become an important technology. Electrically conductive parts are explored using the material Al7075 in the EDM process to produce heat exchangers, anti-wear and gas turbine parts, with its unique advantage in making mold, die, automotive, space and alternative applications, regardless of their hardness, spark and shape. Out a study in manufacturing and their application of alloy are currently being developed for turbine hot section components for both land-based turbines and aircraft engines. The geometrical tolerances were measured by CNC coordinate measuring machining (CMM), model ZEISS Contoura G2, with an accuracy of 4.5 mm [1–3]. Selvarajan [4], Ravinder Kumar [5] explained the Carbon fiber reinforced plastics (CFRPs) and its various applica-tions due to their lightweight and good mechanical properties. However, the machinability of CFRPs is not good due to machining-induced damage [4–5]. Roya [6] studied Differential Reverse Micro Electrical Discharge Machining (RMEDM) is a non-contact thermal micromachining process that is widely used to create high-ratio or multiple 2.5-D features with different intersections as square, circular, triangular. Zhaojun Kou [7] investigated plasma channels were captured by a rapid video camera, which contributed to the elimination of moving electric curves. Mechanical testing was carried out on a titanium alloy basis, which investigated how much higher material removal rate can be easily obtained by moving the arc. Mohan [8] described how material is removed by using a rotary tube, the brass electrode of Al-SiC composite material matrix in electrical discharge machining. Increasing the diameter results in a lower metal removal rate (MRR) and a worse electrode wear rate (EWR). Decreasing the diameter of the brass electrode has improved excellent metal removal rate, better electrode wear rate and surface finish. Bains [9] studied the experimental results improved the surface finish and material

* Corresponding author.
E-mail address: selvalakshmanan86@gmail.com (L. Selvarajan).

Nomenclature

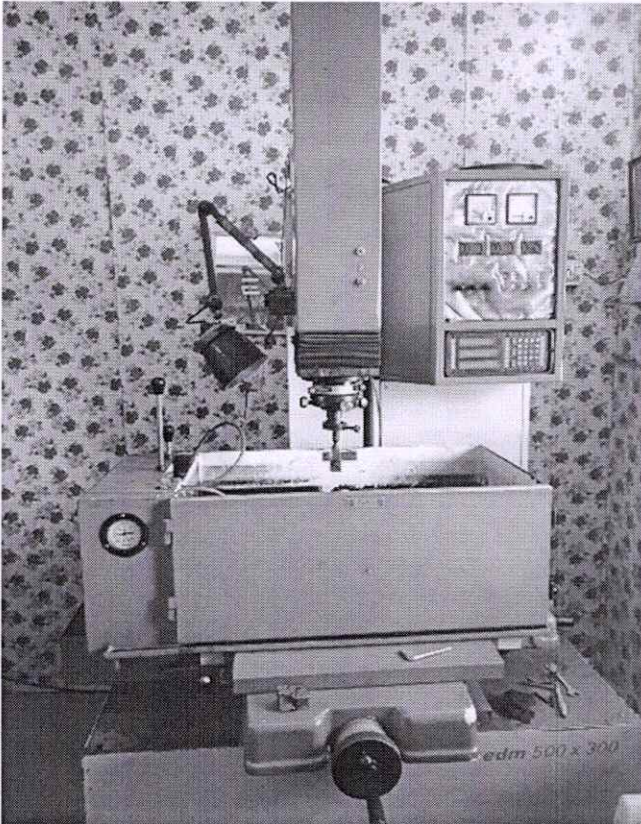|			
EDM	Electrical Discharge Machining	CYL	Cylindricity
MRR	Metal Removal Rate	PER	Perpendicularity
TWR	Tool Wear Rate		
WR	Wear Ratio		
CIR	Circularity		

Fig. 1. Die Sinking Electrical Discharge Machine.

Fig. 2. coordinate Measuring Machine (CMM).

removal ability of the EDM process. Singh [10–12] explained by using 316L stainless steel in presence of TiO_2 nano powder added with electrical discharge machining (PMEDM). It is investigated the surface morphology and chemical composition of the machined particles using electron microscopy and X-ray diffraction methods.

Through a detailed study of the electrical discharge machine of the compounds, it is clear that the impacts on the nature and process of the electrodes are investigated. This research was made possible with the help of its average effective plots of output vol-
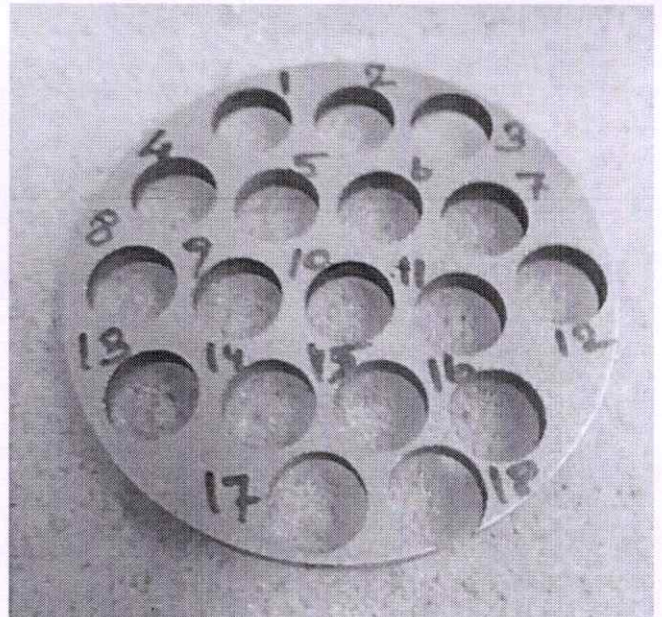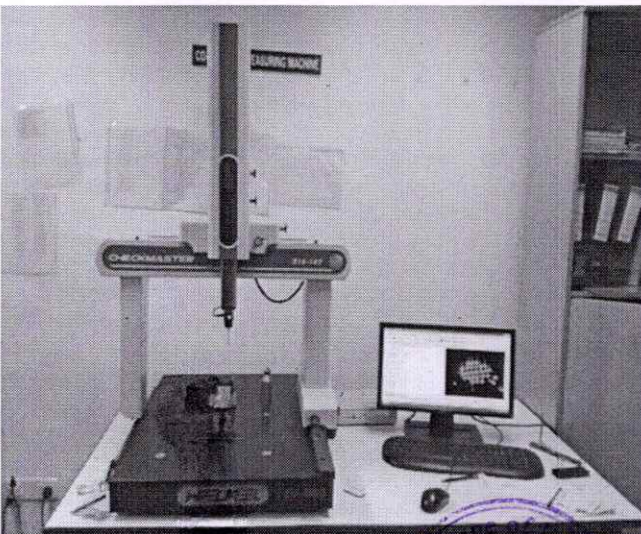

Fig. 3. Al7075 workpiece material.

Table 1
EDM operating conditions for Al7075.

Working condition	Description
Electrode material	Copper
Tool electrode shape	Cu Circle Electrode
Polarity of electrode	Positive
Polarity of the workpiece	Negative
Workpiece	Al 7075
Dimension of the work piece	Dia 50 mm, Thick 4 mm
Dielectric fluid	EDM Oil

Table 2
Factors and levels of EDM.

Symbol	Parameters	Units	Level 1	Level 2	Level 3
A	Current	amp	6	8	10
B	Pulse on time	μs	25	27	29
C	Pulse off time	μs	4	5	6
D	Spark gap	mm	0.2	0.4	0.6
E	Fluid Pressure	kg/cm²	5	10	'15

umes, for all input levels planned for using the mini-tab. Though numerous researches have been attempted in the EDM process, there is limited experimental works done on geometrical tolerances so far.

2. Experimental methodology

Aluminium7075 composite has the highest strength of all the materials. aluminium7075 is used predominantly in highly stressed applications such as trusses, cranes, and bridges. The offers excellent corrosion resistance and has replaced 6061 in many applications. The extruded finish is not as smooth and therefore not as aesthetically pleasing as other metals. The experimental

followed the L_{18} orthogonal array. The machining was done using OSCARMAX'S EDM machine having machining parameters.

The experimental setup of Die Sinking Electrical Discharge Machining is shown in Fig. 1. The coordinate measuring machine (CMM) is shown in Fig. 2. CMM machine is used to measure the value of circularity, cylindricity and perpendicularity. The workpiece material Al7075 is shown in Fig. 3. Table 1 shows the EDM operation conditions for Al7075.Table 2 shows the factors and levels of EDM.

The input parameters are current, pulse on time, pulse off time, fluid pressure, spark gap and shape of the electrode. The corresponding output parameters are machining time, material removal rate, tool wear rate, wear ratio, Geometrical tolerance like circularity, cylindricity and perpendicularity. Table 3 shows the input

Table.3
Input parameters of L_{18} orthogonal array for aluminium material.

S. No	Input Process Parameters					
	Polarity	Current (amp)	Pulse on time (μs)	Pulse off time (μs)	Fluid Pressure (kg/cm²)	Spark gap (mm)
1	Positive	6	25	4	5	0.2
2	Positive	6	27	5	10	0.4
3	Positive	6	29	6	15	0.6
4	Positive	8	25	4	5	0.4
5	Positive	8	27	5	10	0.6
6	Positive	8	29	6	15	0.2
7	Positive	10	25	4	5	0.6
8	Positive	10	27	5	10	0.2
9	Positive	10	29	6	15	0.4
10	Negative	6	25	4	5	0.4
11	Negative	6	27	5	10	0.6
12	Negative	6	29	6	15	0.2
13	Negative	8	25	4	5	0.2
14	Negative	8	27	5	10	0.4
15	Negative	8	29	6	15	0.6
16	Negative	10	25	4	5	0.6
17	Negative	10	27	5	10	0.2
18	Negative	10	29	6	15	0.4

Table.4
Response parameters of experimental result for aluminium material.

S. No	Machining time	MRR	TWR	Wear ratio	Cir	Cyl	Per
	(min)	(g/min)	(g/min)	%	mm	mm	mm
1	15.58	0.0385	0.0019	20.26	0.002	0.026	0.057
2	8.24	0.0752	0.0012	626.66	0.021	0.030	0.042
3	6.29	0.0969	0.0000	No ratio	0.018	0.020	0.033
4	4.32	0.1481	0.0023	64.8	0.008	0.021	0.044
5	3.15	0.1936	0.0000	No ratio	0.009	0.028	0.025
6	4.50	0.1333	0.0022	60.59	0.012	0.027	0.080
7	8.12	0.0751	0.0024	31.29	0.003	0.022	0.206
8	4.39	0.1389	0.0000	No ratio	0.006	0.017	0.010
9	10.01	0.6193	0.0009	68.11	0.004	0.007	0.042
10	33.33	0.0174	0.0003	58.00	0.012	0.016	0.041
11	26.36	0.2276	0.0000	No ratio	0.013	0.022	0.050
12	5.21	0.1190	0.0019	62.30	0.002	0.040	0.080
13	4.03	0.1527	0.0000	No ratio	0.007	0.050	0.125
14	3.32	0.1837	0.0030	61.23	0.005	0.015	0.152
15	5.38	0.1136	0.0000	No ratio	0.008	0.040	0.260
16	2.38	0.1806	0.0000	No ratio	0.009	0.021	0.015
17	11.29	0.1195	0.0088	135.87	0.010	0.032	0.032
18	2.37	0.0464	0.0000	No ratio	0.005	0.015	0.074

The MRR, TWR, WR is studied based on the following expression.
Material Removal Rate (MRR) = $(W_i - W_f)/t$ g/min
Tool Wear Rate (TWR) = $(W_i - W_f)/t$ g/min
Wear Ratio (WR) = WR = MRR/TWR (%)
Where,
W_i - Workpiece initial weight.
W_f - Workpiece final weight.
t - Machining time (min).

parameters of the L_{18} orthogonal array for aluminium material. The L_{18} orthogonal array is based on Design of Experiments (DoE) and is also based on literature survey, it has categorized L_{18} orthogonal array.

3. Results and discussion

The machining time (min), material removal rate (MRR), tool wear rate (TWR), wear ratio (WR) and geometrical tolerance is expressed in Table 4.

Investigated Taguchi's analysis method between the output and input parameters which is shown in the following main consequences plots.

In Fig. 4, maximum material removal rate is obtained for tool-positive, current at level 3 (10 amp), pulse on time at level 3 (29 μs), pulse off time at level 3 (6 μs), fluid pressure at level 3 (15 kg/cm²) and spark gap level 3 (0.6 mm). When current and pulse on time are increased, the material removal rate is improved. While the pulse off time is considered, during 5–15 μs there was an improvement in MRR.

In Fig. 5, minimum electrode wear rate is obtained for current at level 1 (6 amp), pulse on time at level 3 (29 μs), pulse off time at level 3 (6 μs), fluid pressure at level 3 (15 kg/cm²) and spark gap level 3 (0.6 mm). When the current, pulse on time and spark gap are decreased then the tool wear rate is decreased. This plot indicates the x-axis as the value of each input parameter and y-axis as the output values.

In Fig. 6, minimum Circularity is reached when the current is at level 3 (10 amp). Pulse on time at level 1 (25 μs) and pulse off time of level 3 (6 μs) gives minimum circularity is achieved. In the case of spark gap, minimum circularity is obtained in level 3 (0.6 mm). This plot indicates the x-axis as the value of each input parameter and y-axis as the output values. According to this main consequence plot, the optimum conditions for minimum circularity at the current (0.0060 mm), pulse on time, pulse off time, fluid pressure and spark gap are (0.0080 mm).

In Fig. 7, while increasing the pulse on time, pulse off time and fluid pressure at level 3, and using more exit current, the cylindricity can be greatly improved. This plot indicates the x-axis as the value of each input parameter and y-axis as the output values. According to this main consequence plot, the optimum conditions for minimum cylindricity at the current (0.024 mm), pulse on time, pulse off time, fluid pressure and spark gap are (0.023 mm).

In Fig. 8 shows the main consequences plot of perpendicularity in aluminium7075. In order to reduce the perpendicularity, the low
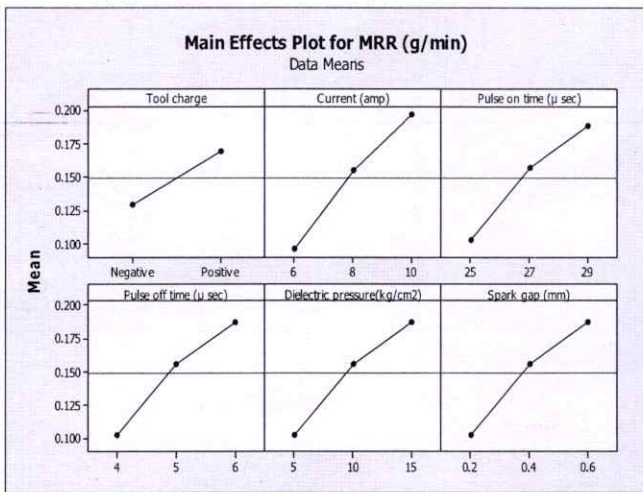

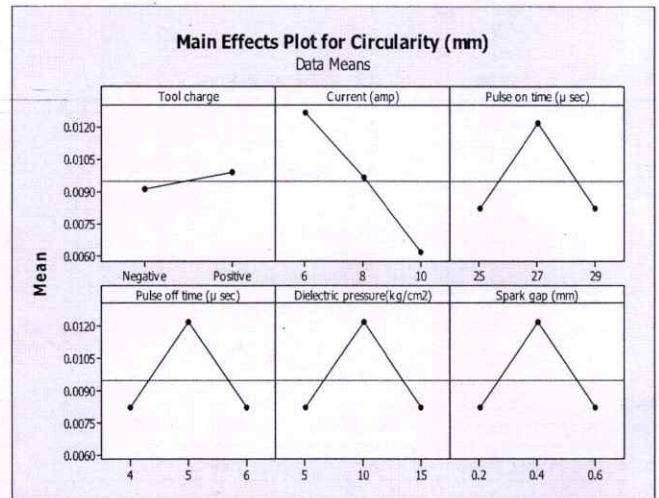Fig. 4. Main consequences plot for metal removal rate.

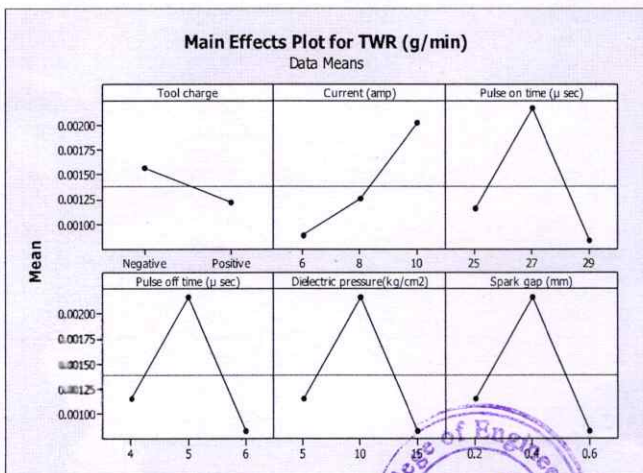Fig. 6. Main consequences plot for Circularity.
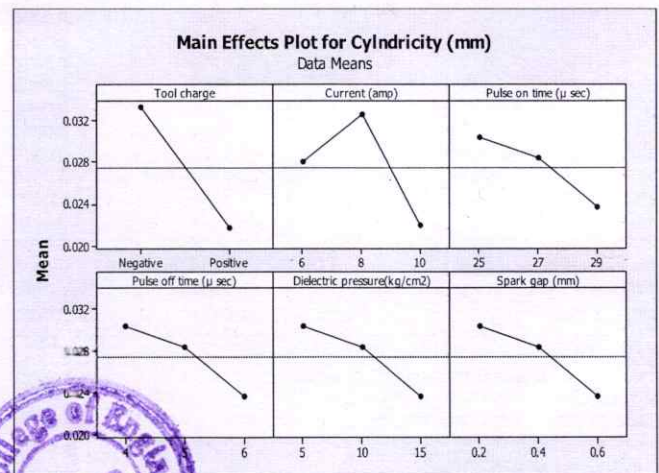

Fig. 5. Main consequences plot for tool wear rate.
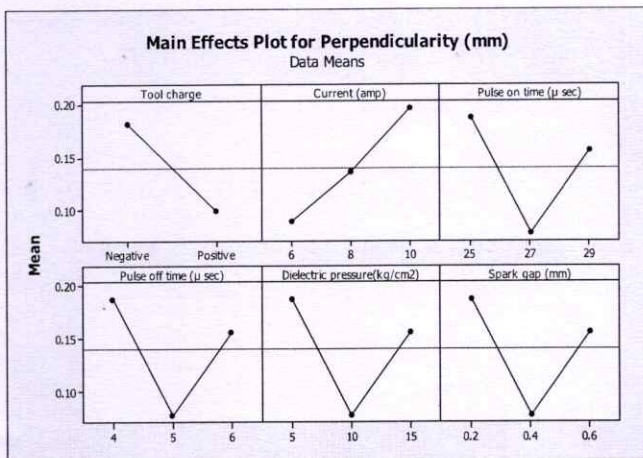

Fig. 7. Main consequences plot for Cylindricity.

Fig. 8. Main consequences plot for Perpendicularity.

discharge current is obtained by applying the moderate pulse on time and the fluid pressure at level 2. This plot indicates the x-axis as the value of each input parameter and y-axis as the output values. According to this main consequence plot, the optimum conditions for minimum circularity at the current (0.08 mm), pulse on time, pulse off time, fluid pressure and spark gap are (0.06 mm).

4. Conclusions

Multiparametric optimization of Al7075 alloy using a copper electrode was used Taguchi relational investigating approach and the following results are express:

- The effect on metal removal rate (MRR) increases when the current (10 amp) and pulse on time (29 μs) is improved, whereas there is not much influence observed when pulse off time (6 μs) is increased and there is very small increase improving the fluxing condition.
- The tool wear rate (TWR) improves when the current (10 amp) and pulse on time (27 μs) is improved at the same time spark gap (0.4 mm) is reduced. Whereas there is no significant change when pulse off time (6 μs) and fluid pressure are improved.
- There is no wear ratio in 3rd, 5th, 8th, 11th, 13th, 15th, 16th, 18th hole.
- The circularity is improved, when the current (10 amp), fluid pressure (5 kg/cm^2), spark gap (0.2 mm) is reduced and pulse off time (27 μs) is increased.
- The cylindricity is enhanced, when the current (10 amp), fluid pressure (15 kg/cm^2) is decreased and pulse off time (5 μs) is

moderate. When the current (6 amp), pulse on time (27 μs) and the spark gap (0.4 mm) is decreased, perpendicularity has improved.

CRediT authorship contribution statement

L. Selvarajan: Writing - original draft, Methodology. **R. Sasikumar:** Conceptualization, Writing - original draft. **N. Senthil Kumar:** Visualization, Investigation. **Prabu Kolochi:** Supervision. **P. Naveen Kumar:** Validation.

Declaration of Competing Interest

The authors declare that they have no known competing financial interests or personal relationships that could have appeared to influence the work reported in this paper.

References

[1] Selvarajan, L., Sathiya Narayanan, C., & Jeyapaul, R. Optimization of Machining Characteristics in EDM of Si3N4-TiN Composites by Taguchi Grey Relational Analysis. In Applied Mechanics and Materials (Vol. 592) (2014): 600-604.
[2] L. Selvarajan, C. Sathiya Narayanan, R. Jeyapaul, Optimization of process parameters to improve form and orientation tolerances in EDM of MoSi2-SiC Composites, Mater. Manuf. Processes 31 (4) (2016) 405–412.
[3] L. Selvarajan, C. Sathiya Narayanan, R. Jeyapaul, Optimization of EDM parameters on machining Si3N4-TiN composite for improving circularity, cylindricity, and perpendicularity, Mater. Manuf. Processes 30 (8) (2014) 954–960.
[4] L. Selvarajan, C. Sathiya Narayanan, R. Jeyapaul, M. Manohar, Optimization of EDM process parameters in machining Si3N4-TiN conductive ceramic composites to improve form and orientation tolerances, Measurement 92 (2016) 114–129.
[5] Ravinder Kumar, Inderdeep Singh, Productivity improvement of micro EDM process by improvised tool, Precis. Eng. 51 (2018) 529–535.
[6] T. Roy, D. Datta, R. Balasubramaniam, Numerical modelling, simulation and fabrication of 3-D hemi-spherical convex micro features using Reverse Micro EDM, J. Manuf. Processes 32 (2018) 344–356, https://doi.org/10.1016/j.jmapro.2018.02.018.
[7] Zhaojun Kou, Fuzhu Han, On sustainable manufacturing titanium alloy by high-speed EDM milling with moving electric arcs while using water-based dielectric, J. Cleaner Prod. 189 (2018) 78–87.
[8] B. Mohan, A. Rajadurai, K.G. Satyanarayana, Electrical discharge machining of Al-SiC metal matrix composites using rotary tube electrode, J. Mater. Proceed. Technol. 153–154 (2004) 978–985.
[9] P.S. Bains, S.S. Sidhu, H.S. Payal, Investigation of magnetic field-assisted EDM of composites, Mater. Manuf. Process. 33 (6) (2018) 670–675, https://doi.org/10.1080/10426914.2017.1364857.
[10] G. Singh, S.S. Sidhu, P.S. Bains, A.S. Bhui, Surface evaluation of EDM machined 316L stainless steel in TiO2 nano-powder mixed dielectric medium, Mater. Today. Proc. 18 (3) (2019) 1297–1303, https://doi.org/10.1016/j.matpr.2019.06.592.
[11] P.S. Bains, S.S. Sidhu, H.S. Payal, Magnetic field assisted EDM: New horizons for improved surface properties, Silicon 10 (2018) 1275–1282, https://doi.org/10.1007/s12633-017-9600-7.
[12] Singh, G., Bhui, A. S., & Singh, M. Analysis of electrical discharge machining parameters for H13 steel using OVAT technique. Engineering Research Express, 1(2), (2019), 025031. DOI: 10.1088/2631-8695/ab52dc.
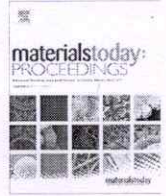
Effects of process parameter on performance measures in electrical discharge machining using copper and brass electrodes

L. Selvarajan [a,*], N. Senthil kumar [a], R. Raja [b], R. Sasikumar [c], V. Muralidharan [d]

[a] Department of Mechanical Engineering, Mahendra Institute of Technology, Namakkal, India
[b] Department of Mechanical Engineering, Gnanamani College of Technology, Namakkal, India
[c] Department of Mechanical Engineering, Mahendra Engineering College (Autonomous), Namakkal, India
[d] Department of Mechanical Engineering, Mahendra Institute of Engineering and Technology, Namakkal, India

ARTICLE INFO

ABSTRACT

In the study of modern-day technology, it's performance and parameters are evaluated using the EDM process in the drilling of stainless steel 316 material. SS316 material is widely used in many industrial applications such as heat transfer process and chemical tank. This test involves testing more material removal rate, improving the material hardness, reducing the electrode wear rate and machining time. The experiment is based on Taguchi L_{18} orthogonal array with 6 levels and 6 parameters like current, dielectric pressure, electrode shape, spark gap, polarity, pulse on and off time. Comparison of copper and brass electrodes in this experiment research is being conducted on how copper electrodes behave differently and exhibit better mechanical performance than brass electrodes. Brass electrode, with its high electrical resistance, low melting point and low thermal conductivity, copper has better performance than brass electrode and the different experimental levels and conditions are investigated.

© 2019 Elsevier Ltd.
Selection and Peer-review under responsibility of the scientific committee of the International Mechanical Engineering Congress 2019: Materials Science.

1. Introduction

Now a days industries require good surface finish in their manufacturing product. When industries start to use the conventional machining process to produce their product, they meet several problems in product like poor surface morphology, low accuracy and material properties changing, etc. To overcome this defect they focus on the use of unconventional machine operation such as EDM. Electrical discharge machine (EDM) has produced the high intensity of spark production in the electrode to remove the material from the workpiece.

2. Literature review

Selvarajan [1] investigation of Si_3-TiN composites are driven by the use of copper electrodes. It is applicable for extrusion dies and balls bearing. It gives good life and effectiveness, but the machining time is high while machining the ceramic composites. Selvarajan [2] optimization of electric discharge machine (EDM) is used

silicon nitride-titanium nitride (Si_3N_4-TiN) ceramic composite to enhance the circularity, cylindricity and perpendicularity. Ceramic composites are mainly used in turbine blades and extrusion dies. This experiment shows the spark process responses are effectively enhancing. Selvarajan [3] studied by using pentagon shaped copper electrode to improve form and orientation tolerance of EN19 alloy material. In this investigation, the design of experiment (DOE) is based on the L_9 orthogonal array. Angularity and Tool wear rate is decreased in the 4th hole. Selvarajan [4] investigation of enhancing geometrical errors using machine material $MoSi_2$-SiC intermetallic composites by analyzing of electrical discharge machining of drilling holes. This technique is very relevant and cost effective for predicting these levels. Selvarajan [5] studied by using the SS316 material alloy and copper electrode, the metal removal rate and the electrode wear rate has improved. Increasing machining voltage, P_{ON} time and decreasing of P_{OFF} time improved MRR. Ravinder Kumar [6] examined the paper, by using improvised tool to improve the micro EDM process productivity. The corresponding characteristics are improved and it requires less fabrication time. Electric discharge drilling aspect ratio is 300% improved compared with solid electrode. Palanisamy [7] investigated that spark sintering is used to prepare the PH stainless steel and then

* Corresponding author.
E-mail address: selvalakshmanan86@gmail.com (L. Selvarajan).
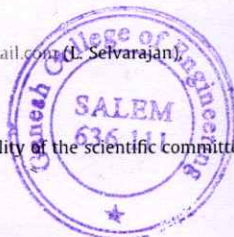
Nomenclature			
MRR	Metal Removal Rate	BH	Brinell Hardness
EWR	Electrode Wear Rate	RH	Rockwell Hardness
WR	Wear Ratio		

analyzed the CNC turning. It gives high hardness value for bending, hardness and toughness. Chengmao [8] evaluated optimization effects on wire cutting electric discharge engine using ceramics composites improve surface integrity. Greater MRR and higher power transistor are used to increase hardness. Palanisamy in his [9] examined the aluminium metal matrix behaviors analyzed by EDM process. Mechanical behaviors of low & high temperature fracture and toughness are identified in aluminium materials. Liu [10] studied the impact of pulse structure on the EDM performance of Si_3N_4-TiN ceramic alloys. This paper describes the influence of Si_3N_4-TiN machining efficiency and material removal mechanism on the EDM discharge pulse pattern Significant differences in material removal, from classical lighting to chemical decomposition, can be seen by applying different pulse systems, such as iso-energy or relaxation discharge types. EDM is centered on Si_3N_4-TiN for the production of ceramic components and the fabrication of the high-temperature mesoscopic gas turbine. By detailed research in literature area of electric discharge machine (EDM) of alloys, it is clear that the effect of the tool and work piece has been thoroughly studied. The results of MRR, EWR and material hardness are analyzed by using main effects plots. In this investigation Taguchi L_{18} orthogonal array with 3 levels and 6 parameters and copper electrode has improved metal removal rate (MRR), hardness and decreasing electrode wear rate (EWR) in various different shapes like circle, square, pentagonal compared to the brass electrode.

3. Materials and methods

In this study, SS316 plate is chosen as a workpiece material. There are three different shapes copper electrode (circle, square, pentagon) are chosen. The parameters which are required for the experiment are arranged by L18 orthogonal array is constructed. Fig. 1 shows the physical setup of Die Sinking Electrical Discharge Machining. Fig. 2 shows the research planes of stainless-steel material through the flow chart. Using copper and brass electrode to machine through holes and measured material SS316 are shown

Fig. 1. Die sinking electrical discharge machine.

in Fig. 3. Table 1 shows the EDM operation and condition for SS316. The thickness of the material and the depth of drilling 2 mm. Table 2 shows the parameters and levels of EDM.

Fig. 4 shows the brass electrode, copper electrode has less tool wear rate and brass electrode has more tool wear rate. So, in this research copper electrode has better performance and stopped brass electrode research. The input parameters are current (amp), P_{ON} time (μs), P_{OFF} time (μs), fluid pressure (kg/cm²), spark gap (mm), polarity and shape of electrodes. The corresponding output parameters are machining time (min), material removal rate (MRR), tool wear rate (EWR), wear ratio (WR), Brinell hardness and Rockwell hardness. Table 3 shows input parameters of L18 orthogonal array for stainless steel material.

4. Results and discussions

Material removal rate, tool wear rate and wear ratio were calculated by using the following formula

$$MetalRemovalRate(MRR) = \frac{(BW - AW)}{T}(g/min),$$

where BW and AW the weights of material before and after machining respectively and T is machining time.

$$ElectrodeWearRate(EWR) = \frac{(EBW - EAW)}{T}(g/min),$$

where EBW and EAW the weight of material before and after machining respectively and T is machining time. The weight of the material and electrode weight is measured by digital weight machine

$$WearRatio(WR) = WR = \frac{MRR}{EWR}(\%),$$

The machine time (min), metal removal rate (MRR), electrode wear rate (EWR), wear ratio (WR), brinell hardness and rockwell hardness is expressed in the Table 4. For the analysis of maximum material removal rate (MRR), machining time (min), tool wear rate (EWR), wear ratio (WR), Brinell hardness and Rockwell hardness studied by the parameters likes voltage (amp), P_{ON} time (μs), P_{OFF} time (μs), fluid pressure (kg/cm²), spark gap (mm), polarity and shape of electrodes. The rockwell and Brinell hardness test are measured in 18 machined experiments respectively, metal's hardness indicates its resistance to permanent shape changes when a compressive force is applied. Metals must often withstand pressure or extreme temperature during its application use, and hardness testing is an ideal way to determine whether the component can perform.

Investigated Taguchi's analysis method between the output and input parameters are shown in the following consequences analysis was carried out minitab software, it is quality control chart statistical.

In the Fig. 5 minimum machining time is obtained for tool-positive, voltage level 2–23 (amp), P_{ON} time at level 3–75 (μ sec), P_{OFF} time at level 2–7 (μ sec), the fluid pressure at level 2–15 (kg cm²), spark gap at level 1 (0.04 mm) and shape at level 3 (Square). The minimum machining time (min) is observed the high pulse on time 75 μ sec. the high concentration of spark produced on time
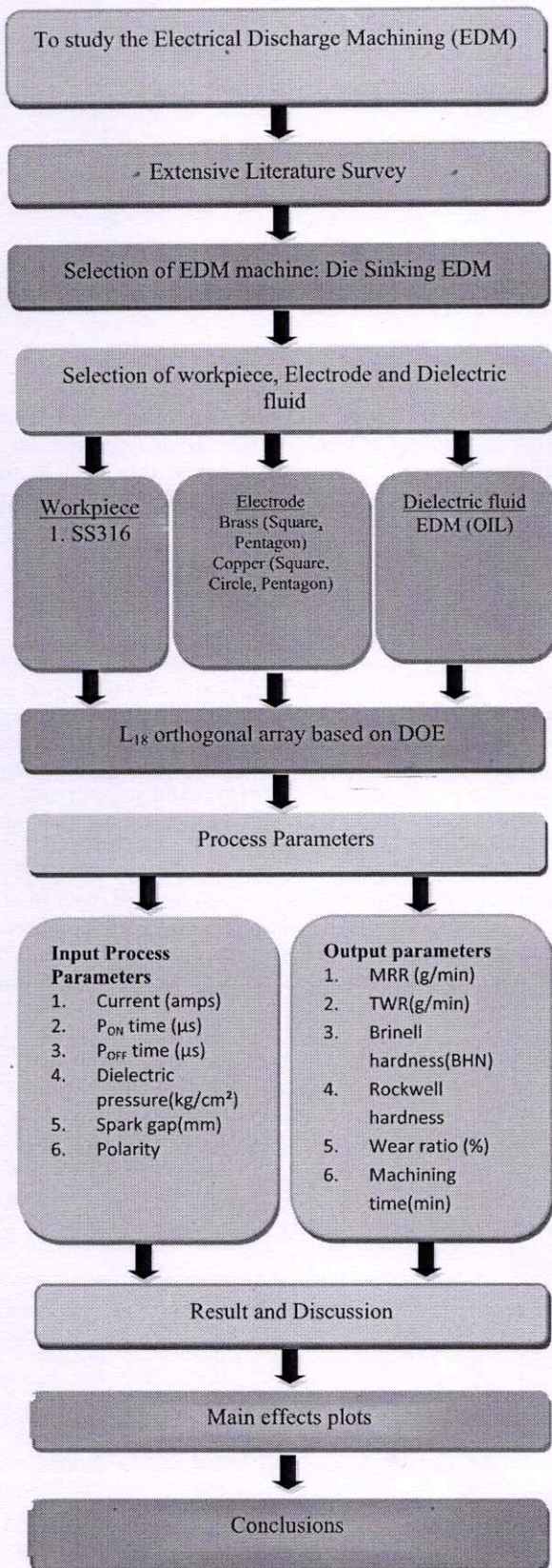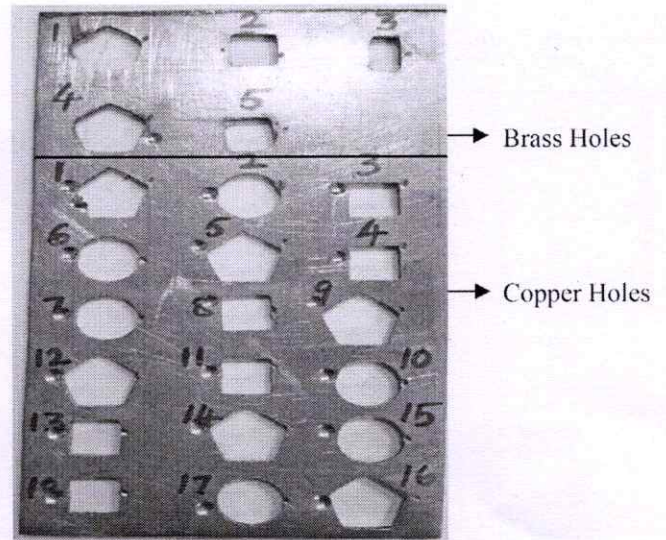
Fig. 2. Research Plan of stainless-steel material.

Fig. 3. SS316 work piece material.

Table 1
EDM operation and conditions for SS316.

Working conditions	Description
Electrode material	Copper electrode
Dimension of hole	5 mm (Each Side)
Depth of drilling	2 mm
Workpiece polarity	Negative
Type of current	DC Power Supply
Specimen Material	SS316 Stainless Steel
Discharge current (I, A)	21–25amps
Pulse on time (ton, μ s)	35–75 μs
Pulse off time (t off, μ s)	4–9 μs
Dielectric fluid	EDM oil
Fluid pressure (kg/cm2)	10–20 kg/cm^2
Spark gap (mm)	0.02–0.06 mm

In the Fig. 6 maximum material removal rate is obtained for tool-positive, voltage level 3 (25 amp), P_{ON} time at level 1 (35 μ sec), P_{OFF} time at level 3 (9 μ sec), the fluid pressure at level 1 (10 kg cm^2) and spark gap at level 3 (0.06 mm). Maximum MRR is observed at high peak current of 25 A and pulse off time 9 μ sec. The high concentration of discharge energy in the spark gap leads to the rapid melting and evaporation of the metal. The pentagon-shaped electrode is obtained the more metal removal rate (MRR) in the 7th experiment there is no significant changes in the pulse on time, fluid pressure and spark gap.

In the Fig. 7 minimum tool wear rate is obtained for tool-negative, voltage level 1 (21 amp), P_{ON} time at level 2 (55 μ sec), P_{OFF} time at level 2 (7 μ sec), the fluid pressure at level 2 (15 kg cm2), spark gap at level 3 (0.06 mm) and shape at level 1 (Circle). The minimum tool wear rate (TWR) is obtained at increase of spark gap 0.06 mm and P_{ON} is reduced the tool material eroded value, the lower Electrode Wear Rate (EWR) on the 12th experiment. The voltage, P_{OFF} and fluid pressure which is turn eroded the more tool material.

In the Fig. 8 minimum wear ratio is obtained for tool-positive, voltage level 3 (25 amp), P_{ON} time at level 1 (35 μ sec), P_{OFF} time at level 2 (7 μ sec), the fluid pressure at level 3 (20 kg cm2), spark gap at level 1 (0.02 mm) and shape at level 3 (Square). The zero-wear ratio (TWR) is observed that tool wear is affected by the precipitation of carbon from the hydrocarbon dielectric on the electrode surface during sparking characteristics of P_{OFF}, P_{ON} and spark gap are decreased with the fluid pressure and voltage is increase the minimum wear ratio is obtained.

leads to the rapid machining process of the metal. The minimum machining time (min) of the square-shaped electrode is obtained in the 5th experiment there is no significant changes in the machining voltage, P_{OFF}, fluid pressure and spark gap.

Table 2
Limits and levels of EDM.

Symbol	Parameters	Units	Level 1	Level 2	Level 3
A	Current	amp	21	23	25
B	Pulse on time	μs	35	55	75
C	Pulse off time	μs	4	7	9
D	Spark gap	mm	0.02	0.04	0.06
E	Dielectric pressure	Kg/cm^2	10	15	20
F	Shape of electrode	–	Circle	Circle	Circle
			Square	Square	Square
			Pentagonal	Pentagonal	Pentagonal
G	Polarity	–	Straight polarity	Straight polarity	Straight polarity
			Reverse polarity	Reverse polarity	Reverse polarity

Fig. 4. After machining brass electrodes.

In the Fig. 9 maximum brinell hardness is obtained for tool-positive, voltage level 1 (21 amp), P_{ON} time at level 2 (55 μ sec), P_{OFF} time at level 2 (7 μ sec), the fluid pressure at level 1 (10 kg cm^2), spark gap at level 1 (0.02 mm) and shape at level 1 (Circle). The Brinell hardness is studied that voltage, P_{OFF}, P_{ON}, fluid pressure and spark gap are decreased the maximum hardness value is obtained, the maximum resistance value is achieved in 5th experiment.

In the Fig. 10 maximum rockwell hardness is obtained for tool-positive, voltage level 3 (25 amp), P_{ON} time at level 1 (35 μ sec),

P_{OFF} time at level 1 (4 μ sec), the fluid pressure at level 2 (15 kg cm^2), spark gap at level 2 (0.04 mm) and shape at level 1 (Circle). The Rockwell hardness is observed that fluid pressure and spark gap are decreased and the voltage is increasing the maximum resistance to be achieved in 9th and 3th experiments there is no significant changes in the P_{ON}, P_{OFF}.

5. Conclusions

Finally, comparison of copper and brass electrodes in this experiment and the research is being conducted on how copper electrodes a behave differently and exhibit better mechanical performance than brass electrodes. Improving the metal removal rate (MRR), reduced electrode wear rate (EWR) and machining time (min) by using copper electrode. The effect and efficiency for each of the input levels in the output attributes were analysed accurately by using the trend of the graph.

- The minimum machining time (min) is observed the high pulse on time 75 μ sec. the high concentration of spark produced on time leads to the rapid machining process of the metal. The minimum machining time 4.05 min achieved in the 5th experiment of square-shaped electrode.
- Maximum MRR is observed at high peak current of 25 A and pulse off time 9 μ sec. The high concentration of discharge energy in the spark gap leads to the rapid melting and evaporation of the metal. The pentagon-shaped electrode is achieved the more metal removal rate (MRR) in the 7th experiment.

Table 3
Input parameters of LI8 orthogonal array for stainless steel material.

Exp. no	Input process parameters						
	Polarity	Current (amp)	Pulse on time (μs)	Pulse off time (μs)	Dielectric pressure (kg/cm^2)	Spark gap	Shape
1	POSITIVE	21	35	4	10	0.02	SQUARE
2	POSITIVE	21	55	7	15	0.04	PENTAGONAL
3	POSITIVE	21	75	9	20	0.06	CIRCLE
4	POSITIVE	23	35	4	15	0.04	CIRCLE
5	POSITIVE	23	55	7	20	0.06	SQUARE
6	POSITIVE	23	75	9	10	0.02	PENTAGONAL
7	POSITIVE	25	35	7	10	0.06	PENTAGONAL
8	POSITIVE	25	55	9	15	0.02	CIRCLE
9	POSITIVE	25	75	4	20	0.04	SQUARE
10	NEGATIVE	21	35	9	20	0.04	PENTAGONAL
11	NEGATIVE	21	55	4	10	0.06	CIRCLE
12	NEGATIVE	21	75	7	15	0.02	SQUARE
13	NEGATIVE	23	35	7	20	0.02	CIRCLE
14	NEGATIVE	23	55	9	10	0.04	SQUARE
15	NEGATIVE	23	75	4	15	0.06	PENTAGONAL
16	NEGATIVE	25	35	9	15	0.06	SQUARE
17	NEGATIVE	25	55	4	20	0.02	PENTAGONAL
18	NEGATIVE	25	75	7	10	0.04	CIRCLE

Table 4
Response parameters of Experimental Result for stainless steel materials.

Exp.no	Workpiece weight (g)		Tool weight (g)		Machining time	MRR	EWR	Wear ratio	Rockwell hardness	Brinell hardness
	BW	AW	EBW	EAW	(min)	(g/min)	(g/min)	%	–	BHN
1	68.5	68.07	14.98	14.93	5.04	0.085	0.009	9.46	48	144
2	68.07	67.37	19.04	19	6.48	0.108	0.003	36	46	143.6
3	67.37	66.22	13.68	13.66	5.4	0.212	0.003	70.66	49	143.2
4	66.22	65.58	13.66	13.64	6.1	0.104	0.003	34.66	85	143.2
5	65.58	65.23	14.93	14.9	4.05	0.086	0.007	12.28	39	144.5
6	65.23	64.44	19	18.93	6.24	0.126	0.011	11.45	35	144
7	64.44	63.47	18.93	18.9	4.37	0.221	0.006	36.83	40	143.2
8	63.47	62.84	13.64	13.62	4.2	0.15	0.004	37.5	28	144
9	62.84	62.58	14.9	14.86	4.28	0.06	0.009	6.66	54	142.8
10	62.58	61.53	18.9	18.77	44.42	0.023	0.002	11.5	38	144
11	61.53	60.85	13.62	13.59	46.8	0.014	0.0006	23.33	32	143.6
12	60.85	60.31	14.86	14.85	41.5	0.013	0.0002	65	34	143.6
13	60.31	59.62	13.59	13.5	42.32	0.016	0.002	8	37	143.2
14	59.62	59.14	14.85	14.84	39.62	0.012	0.0002	60	29	142.4
15	59.14	58.58	18.77	18.76	38.47	0.014	0.0002	70	28	143.2
16	58.58	58.14	14.84	14.81	42.65	0.01	0.0007	14.28	41	142.8
17	58.14	57	18.76	18.69	43.72	0.026	0.001	26	44	142.4
18	57	56.66	13.5	13.46	40.25	0.008	0.0009	8.88	46	143.6
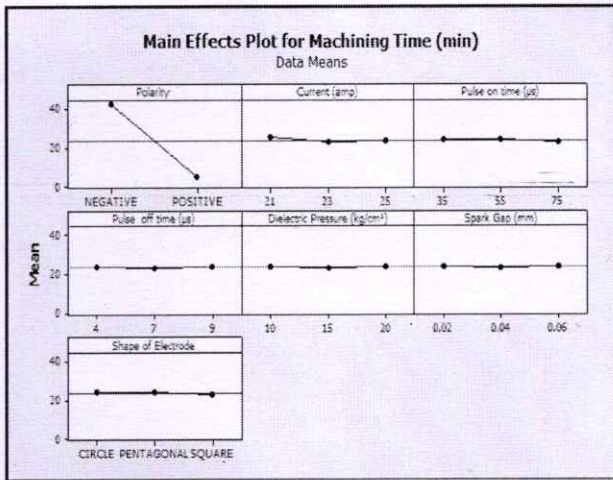
Fig. 5. Main consequences plot for machining time.
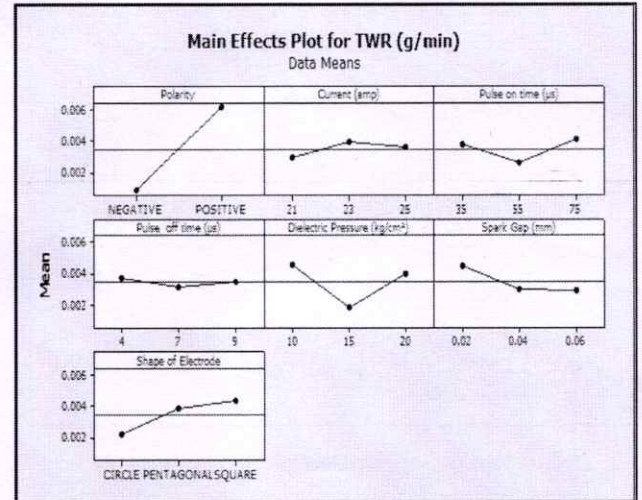
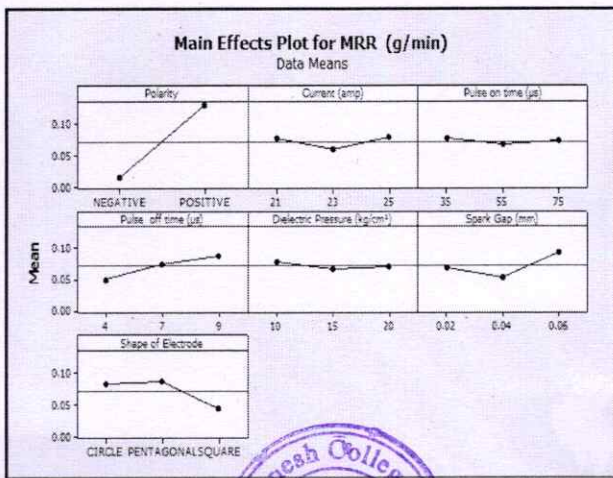**Fig. 7.** Main consequences plot for tool wear rate.

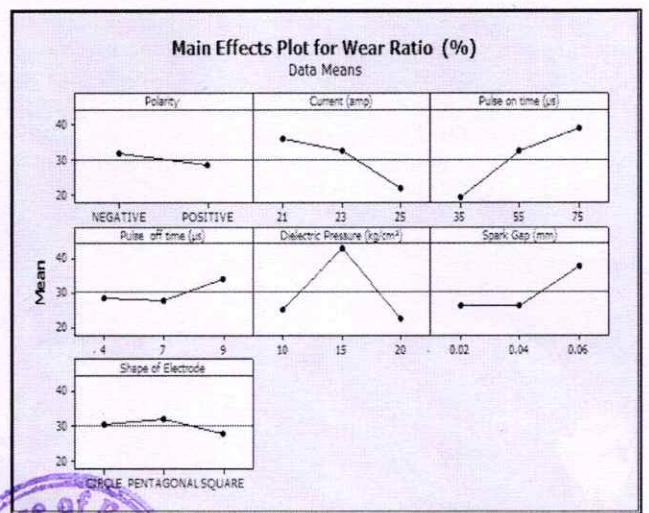**Fig. 6.** Main consequences plot for metal removal rate.
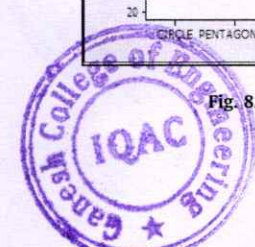

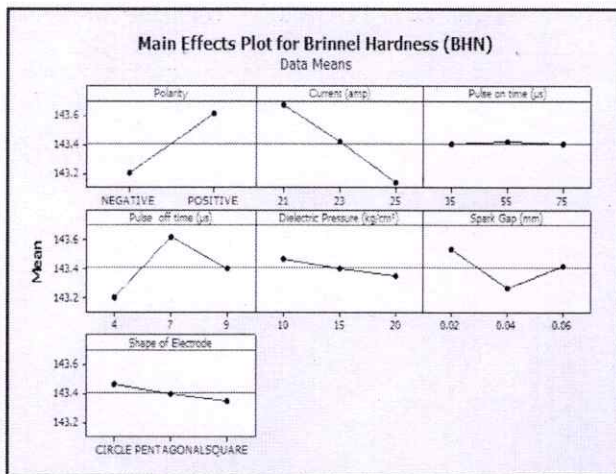**Fig. 8.** Main consequences plot for wear ratio.

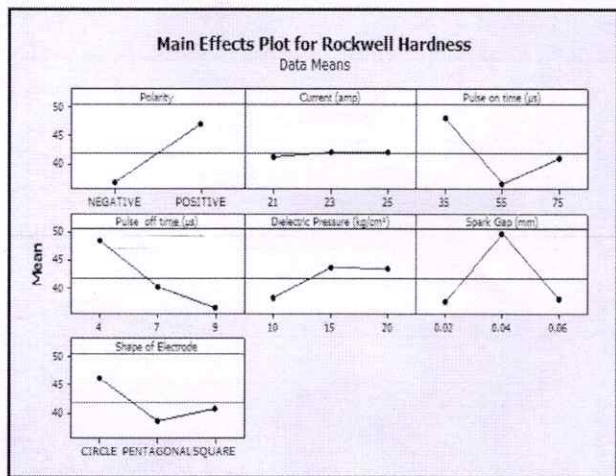**Fig. 9.** Main consequences plot for Brinell hardness test.

Fig. 10. Main consequences plot for Rockwell hardness test.

- The minimum tool wear rate (TWR) is obtained at increase of spark gap 0.06 mm and P_{ON} is reduced the tool material eroded value, the lower Electrode Wear Rate (EWR) is achieved in 12th experiment of square shape electrode. The voltage, P_{OFF} and fluid pressure which is turn eroded the more tool material.
- Sparking characteristics of P_{OFF}, P_{ON} and spark gap are decreased with the fluid pressure and voltage is increase the minimum wear ratio is obtained. There is less wear ratio in 1st, 5th, 9th, 16th hole (Square shape), 6th, 10th hole (Pentagonal shape), 13th, 18th hole (Circle hole).

- The Brinell hardness is studied that voltage, P_{OFF}, P_{ON}, fluid pressure and spark gap are decreased the maximum hardness value is obtained, the maximum resistance value is achieved in 5th experiment and the Rockwell hardness is observed that fluid pressure and spark gap are decreased and the voltage is increasing the maximum resistance to be achieved in 9th and 3th experiments.

CRediT authorship contribution statement

L. Selvarajan: Writing - original draft, Methodology. **N. Senthil kumar:** Conceptualization, Writing - original draft. **R. Raja:** Visualization, Investigation. **R. Sasikumar:** Writing - review & editing, Supervision. **V. Muralidharan:** Methodology, Project administration, Validation.

Declaration of Competing Interest

The authors declare that they have no known competing financial interests or personal relationships that could have appeared to influence the work reported in this paper.

References

[1] L. Selvarajan, M. Manohar, P. Dhinakaran, Modelling and experimental investigation of process parameters in EDM of Si₃N₄-TiN composites using GRA-RSM, J. Mech. Sci. Technol. 31 (1) (2017) 111–122.
[2] L. Selvarajan, C. Sathiya Narayanan, R. Jeyapaul, M. Manohar, Optimization of EDM process parameters in machining Si₃N₄–TiN conductive ceramic composites to improve form and orientation tolerances, Measurement 92 (2016) 114–129.
[3] L. Selvarajan, D. Katherasan, B. Srivijai, R. Rajavel, M. Ramamoorthi, Experimental analysis of EN 19 alloy material on EDM for improving geometrical errors using copper pentagon shaped electrode, Mater. Today:. Proc. 5 (2018) 4508–4514.
[4] L. Selvarajan, C. Sathiya Narayanan, R. Jeyapaul, Optimization of EDM hole drilling parameters in machining of MoSi₂-SiC intermetallic/composites for improving geometrical tolerances, J. Adv. Manuf. Sys. 14 (04) (2015) 259–272.
[5] L. Selvarajan, R. Rajavel, P. Gopi, M. GokulKumar, N. Kasthuri, Investigation on EDM of SS316 alloy material using copper electrode for improving MRR and TWR. J. Manuf. Eng. 13 (2018) 142–147.
[6] Ravinder Kumar, Inderdeep Singh, Productivity improvement of micro EDM process by improvised tool, Precision Eng. 51 (2018) 529–535.
[7] D. Palanisamy, A. Devaraju, S. Harikrishnan, N. Manikandan, Machinability studies on CNC turning of PH stainless steel with coated inserts, Mater. Today: Proc. 5 (6) (2018) 14520–14525.
[8] Chengmao Zhang, Effect of wire electrical discharge machining (WEDM) parameters on surface integrity of nanocomposite ceramics, Cer. Int. 40 (7) (2014) 9657–9662.
[9] D. Palanisamy, A. Devaraju, N. Manikandan, K. Balasubramanian, D. Arulkirubakaran, Experimental investigation and optimization of process parameters in EDM of aluminium metal matrix composites, Mater. Today: Proc. (2019).
[10] K. Liu, D. Reynaerts, B. Lauwers, Influence of the pulse shapeon the EDM performance of Si3N4–TiN ceramic composite. CIRP Ann. – Manuf. Technol. 58 (2010) 217–220.

Design and Finite Element Analysis of a Concentric Tube Heat Exchanger

S. SIVAKUMAR[1], M.B. TAMILARASAN[2], J. SHARAN[3], S. LOGANATHAN[4]

[1] Assistant Professor, Department of Mechanical Engineering, Ganesh College of Engineering, Mettupatti, Salem, Tamilnadu, India

[2,3,4] U. G Student, Department of Mechanical Engineering, Ganesh College of Engineering, Mettupatti, Salem, Tamilnadu, India

Abstract - Heat exchangers are essential in many sectors, such as paper, chemicals, oil, processing, petroleum refining, and power plants. The need for efficient heat exchangers is a result of their high efficiency and environmental concerns. Heat transfer improvement is crucial for increasing efficiency since it enables smaller heat exchanger sizes and a high heat transfer rate with less space needed. Using plain tube and plain twisted tape inserts, counterflow heat exchangers enhance the transfer of heat properties of concentric tube heat exchangers. To improve heat transmission & generate turbulence, twisted tape inserts are used to concentric tube heat exchangers. A variety of techniques, such adding fins or raising fluid velocity, can be tested to see which improves heat transmission in small heat exchangers the most.

Index Terms- Heat transfer, Petroleum refining, Efficiency, Counter flow, Concentric tube, Plain and Twisted tape.

I. INTRODUCTION

The concentric pipe heat exchanger is a method for transferring heat among the two fluids without mixing at different temperatures. It makes use of convection and conduction, with conduction passing through the walls of the heat exchanger and convection happening in each fluid. Chemical facilities and fossil fuel refineries are two examples of industrial domains where tube inserts are utilised to facilitate heat transmission. Heat exchangers frequently experience cross-, parallel-, and counterflow flow patterns. The most efficient technique is counterflow, which has warm fluid entering at one end and cold fluid leaving at the same end. Because of its efficiency, it is the most often used kind of fluid-to-fluid heat exchanger. The literature examines concentric tube heat exchanger design using both an analytical and numerical method.

Pragneshkumar et al. [1] aim to enhance heat transfer surfaces in engineering applications such as air conditioning, heat exchangers, chemical reactors, and refrigeration systems. Passive heat transfer methods, like twisted tape, are important because they improve the effective surface area interaction with fluids. When a quadratic turbulator was linked to a twisted tape insert, the study's double pipe counter flow heat exchanger outperformed a basic twisted tape insert in terms of performance ratio, increasing from 1.13% to 1.16%. In transfer of heat and technical applications, such as heat exchangers, vehicles, & thermal power plants, cylinder pipes are frequently utilised. Heat may be transferred through three different methods: conduction, convection, and radiation. With an emphasis on parallel flow concentric tube heat exchangers, the heat transmission and friction factor in circular tube channels with and without inserts are investigated by Kanika et al. [2]. The primary cause of the heat transfer effect is induced turbulence. which raises the heat transfer rate. With the same shape, various latitudinal spacings, such as $y = 15$ and $y = 45$, provide different outcomes under different mass flow rates and heat conditions. The study discovered that the quality of heat transfer characteristics for variables including friction factor, pressure drop, Re, and Nu declines with increasing distance. In comparison to $y = 45$, the best outcomes were obtained with a linear geometrical spacing of $y = 15$.

The efficiency of heat exchangers depends on the heat transfer rate, hence new methods for increasing it are required. Techniques for improving passive heat transmission are recommended since they don't impact the system's performance as a whole. Industries employ twisted tape inserts extensively because of their low setup costs, simplicity of maintenance, and affordability. Kalapala et al. [3] look at the effectiveness of a dual pipe heat exchanger system with twisted tape inserts. The study is conducted for different mass flow rates and input temperatures for both parallel and counterflow configurations. The data indicates that the heat exchanger performs better in a counter flow architecture with twisted tapes than in a parallel flow design with twisted plates. The continuous temperature differential across the cross section makes counterflow more effective than parallel flow. Because twisted tape inserts create turbulence in the hot fluid moving zone, they also boost efficacy. Twisted tapes are shown to boost efficacy by 30% at low mass flow rates.

Bandu et al. [4] studied the performance of double pipe heat exchangers (DPHEs) in oil refinery and

other large chemical processes. They investigated the flow and temperature field inside the tubes and created DPHEs with various fin orientations. For six distinct fin inclinations, they examined the impacts and heat transmission properties of DPHEs (0, 5, 10, 10). The study used CATIA V5 and hyper mesh for meshing, and ANSYS FLUENT R18.0 for studying the flow and temperature field inside the tubes. The study found that helical fins improved the heat transfer rate and overall coefficient of heat transfer.

Using ZnO nanofluid, Vijaya Sagar et al [5] studied the heat transfer and friction factor of a twin pipe heat exchanger. It was discovered that twisted tape containing 0.4% ZnO nanofluid raised the Nu by 23.56% and the friction factor by 15.32%. Research on the properties of heat transmission in a helically coiled heat exchanger was carried out by Jayakumar et al [6]. They discovered that modelling real heat exchangers with constant temperature or heat flow boundary conditions was insufficient. Rather, they used temperature-dependent features of the heat transport medium and conjugate heat transfer to analyse the heat exchanger. A correlation was built to ascertain the interior heat transfer coefficient, and an experimental setup was established to assess heat transfer qualities. According to studies by Yamini et al. [7] helical coil-tube heat exchangers are being looked at for use in a variety of manufacturing due to their more compact design, larger heat transfer area, and improved heat transfer capabilities. According to the study, the intricate flow pattern of helically coiled tubes results in increased heat transfer rates compared to straight tubes. The significance of different curvature ratios and geometry in heat transfer is further highlighted by the research. The optimal fin No for maximum wall temperature and heat transfer was found to be 10. Triangular-shaped fins had the least amount of wall temperature dispersion, according to the study. Technologies for improving heat transmission are critical to industries including electronic components, petrochemicals, industrial processes, and thermal power plants.

Although millimetre or micron-sized particles, which can lead to settling, surface abrasion, and clogging in heat transfer equipment, have received the majority of study attention, energy transmission fluids with suspended solid particles have also been investigated to enhance heat transfer. According to research by Rao et al [8] convective heat transfer in transition flow is greatly enhanced when Al_2O_3 nanoparticles are used as a dispersed phase in water. This improvement increases with Reynolds number and particle concentration.

Deepak et al [9] focuses on employing plain tube, helical fins and plain tube with helical fins with inserts to improve thermal performance in a twin

pipe heat exchanger. An insert on the helical fins increases turbulent intensity, which boosts heat transmission. To examine the flow of heat between two liquids via a solid barrier, Joshua [10] created a concentric tube heat exchanger. (LMTD) approach was used, and the apparatus was built for a counter-flow configuration. Water was used in the experiment, hot and cold water were given at 87°C and 27°C, respectively. Hot water came out at 73°C, while chilly water came out at 37°C. With an overall heat transfer coefficient of 711 W/m²K and a 48°C log, the heat exchanger was 73.4% efficient. The design of a double pipe heat exchanger in a chemical plant is examined by Karthik et al. [11] With hot water in the outer pipe and hot oil in the inner pipe, the heat exchanger is built to withstand real-world working circumstances. (LMTD) technique and the effectiveness-number of transfer units (ϵ-NTU) approach were employed in an analytical model. To characterise the heat exchanger's performance in terms of important dimensionless metrics, performance charts were created. For the design study, both counterflow and parallel flow topologies were taken into account. Another option was a numerical model. Based on the criteria and inputs that are available, designers may select an acceptable design process by using the findings, which demonstrate that both analytical and numerical approaches provide the same outcomes.

Pichandi [12] talks about the significance of heat transfer in heat exchangers, emphasising the effect of entropy generation on operating parameters and shape. A MATLAB code is created to solve the mathematical model, which is based on the 1st & 2nd laws of thermodynamics. For the parameters employed in the study, an experimental setup is created, and the model and code are verified with the help of the experimental findings. In addition, a numerical test for grid independence is conducted, and the ideal Re for the specified shape and operating conditions is discovered.

II. DESIGN OF CONCENTRIC TUBE

This project uses SolidWorks software to create a model of this heat exchanger. The model will be used to simulate and optimise the performance of the heat exchanger design. This project includes three distinct types of tubes.
- Normal plain tube
- Plain tape inserted
- Plain Twisted Tape Insert

A. Normal Plain Tube
A concentric tube heat exchanger is a system consisting of two smaller tubes used to exchange heat. It can generate turbulent conditions at low flow rates and withstand high pressure operations, which

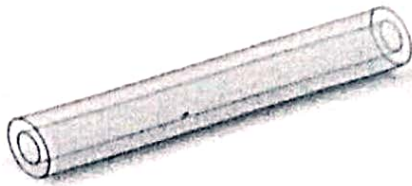raises the rate of heat transfer and coefficient of heat transfer.

Fig. 1 Normal Plain Tube

B. Plain Tape Inserted Tube

Straight tape inserts have a mean heat transfer gain of 4-24% associated to plain tubes, mainly due to their robust turbulence intensity, which enhances heat transfer. However, this can also result in higher pressure drop and increased energy consumption. The cost of implementing and maintaining these inserts may outweigh the benefits of slightly improved heat transfer.
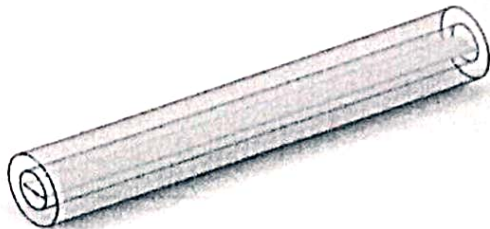

Fig. 2 Plain tape inserted

C. Plain Twisted Tape Insert

Twisted tape and longitudinal tubes are passive equipment that enhance heat transfer rates. Twisted tape generates swirl flow, improving fluid mixing and reducing resistance near the wall. Tubes with longitudinal inserts are also effective for improving heat transfer. Perforated double counter twisted tape inserts in a circular tube increased heat transfer by 80–29% compared to a plain tube, according to a study. This suggests that using twisted tape and longitudinal tubes in tubes can be a practical and efficient method for improving heat transfer in various applications. Overall, the use of these passive equipment options can lead to energy savings and improved overall system performance in a variety of applications.

Fig. 3 Plain Twisted Tape Insert

The precise parametric parameters, including length, breadth, thickness, inner diameter, and outer diameter of the chosen concentric tube, are shown in Table 1 below. This data is essential for correctly simulating the fluid flow inside the tube and figuring out the mechanical characteristics of the tube.

Table. 1 Geometry Conditions

PARAMETERS	INNER PIPE	OUTER PIPE	PLAIN TAPE
Length	800mm	800mm	800mm
Inner diameter	66mm	126mm	-
Outer diameter	70mm	130mm	-
Width	-	-	50.8mm
Thickness	2mm	2mm	3mm

III.   MATERIAL PROPERTIES

The Concentric tube has selected according to the parameters taken as shown below. The inner pipe, outer pipe and insert are available in market for that material as well as its dimensions. Table 2 represents the mechanical properties of the concentrated pipe, and Table 3 represents the different parametric properties of the cold water and hot water.

Table. 2 Material Property

Material	Aluminum
Thermal Conductivity	202.4 (w^{mk})
Specific Heat	871 (j^{kgK})
Density	2719 (kg^{-m3})

Table. 3 Hot & Cold-Water Properties

Description	Cold Water (20 °C)	Hot Water (70 °C)	Symbol
Thermal Conductivity	0.614	0.654	(w^{mk})
Density	995.215	983.2	(kg^{-m3})
Specific Heat	4180.15	4184.3	(j^{-1kg})
Viscosity	0.000827	0.000466	(kg^{-1ms})

IV.   ANALYSIS OF CONCENTRIC TUBE HEAT EXCHANGER
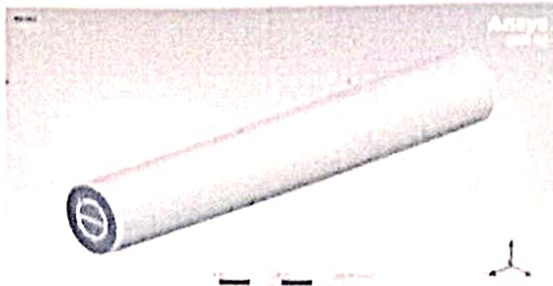

Fig. 4 Normal Tube Model in ANSYS software

Fig. 5 Plain and Twisted Tape Model in ANSYS software

ANSYS offers the perfect option for everyone from professionals trying to simulate complicated materials and non-linear behaviour to designers and infrequent users seeking quick and reliable results. ANSYS Mechanical's user-friendly interface allows engineers of any level of experience to obtain accurate and timely results. Figure 4 represents a simple concentric tube heat exchanger model in which there are no hidden features, but both the plain tape and the twisted tape inserted in Figure 5 are hidden in the concentric tube heat exchanger model.

Any model may be effortlessly fitted with the optimal mesh thanks to ANSYS Mechanical's intelligent mesh technology. Astute algorithms generate high-quality models automatically and also simplify the process of adding controls for any last-minute adjustments that may be required.

A. Meshing
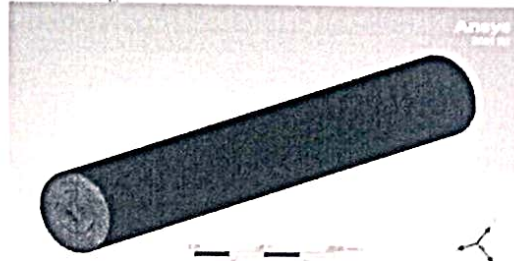
Fig. 6 Mesh Generation of Normal Tube Model
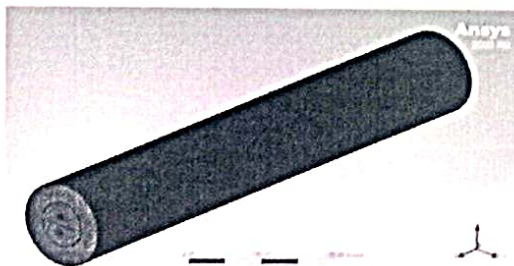
Fig. 7 Mesh Generation of Plain and Twisted Tape Model

Figure 6 shows a simple concentric tube heat exchanger mesh model without hidden features, while Figure 7 shows both plain tape and twisted tape inserted mesh models hidden within the concentric tube heat exchanger model.

V. RESULT & DISCUSSION

A. Normal Tube Model
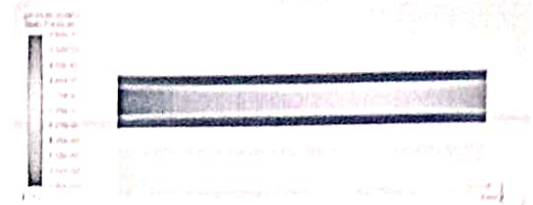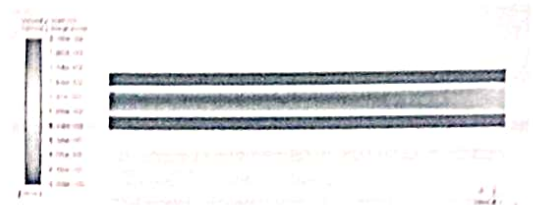

Fig. 8 Pressure Contour Results of Normal Tube

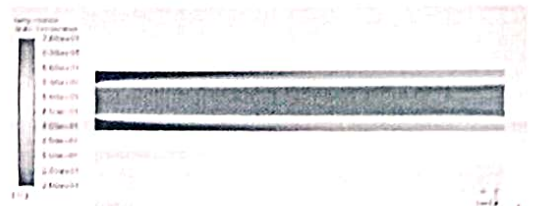Fig. 9 Velocity Contour Results of Normal Tube

Fig. 10 Temperature Contour Results of Normal Tube

Fig. 11 Temperature Results of Normal Tube

Figures 8, 9, and 10, respectively, display the pressure, velocity, and temperature contour findings of a conventional tube concentric heat exchanger. Figure 11 reports the temperature results at both the inlet and outlet regions of the heat exchanger, providing a comprehensive overview of the thermal performance. These illustrations are essential for comprehending the exchanger's heat transfer mechanism and can point out possible areas for

improvement. Analysing these temperature profiles can help identify any inefficiencies or areas where adjustments may be necessary to optimize heat transfer.

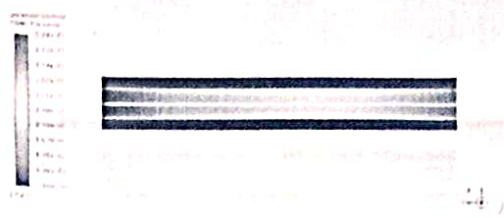### B. Plain Tape Model

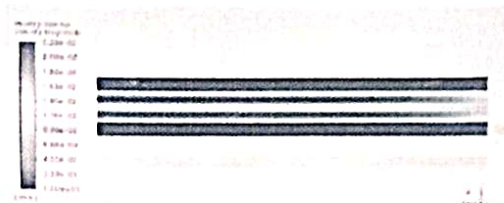Fig. 12 Pressure Contour Results of Plain Tape Concentric Tube

Fig. 13 Velocity Contour Results of Plain Tape Concentric Tube
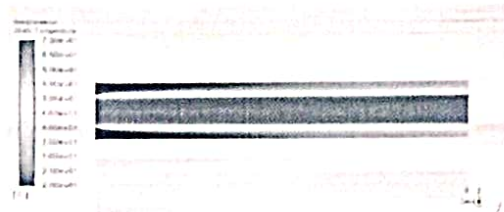

Fig. 14 Temperature Contour Results of Plain Tape Concentric Tube

Fig. 15 Temperature Results of Plain Tape Concentric Tube

The pressure, velocity, and temperature contour results of a simple tape concentric tube heat exchanger is shown in Figures 12, 13, and 14, respectively. The temperature readings at the heat exchanger's intake and exit areas are shown in Figure 15, which offers a thorough summary of the thermal performance. These diagrams can highlight potential areas for improvement and are crucial for understanding the heat transfer process of the

exchanger. These temperature profiles may be analysed to find any inefficiencies or places where changes could be needed to maximize heat transmission.

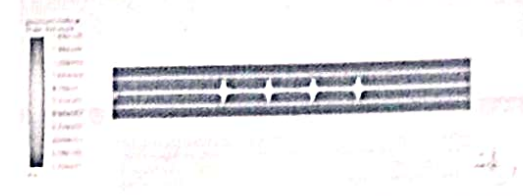### C. Twisted Tape Model

Fig. 16 Pressure Contour Results of Twisted Tape Concentric Tube

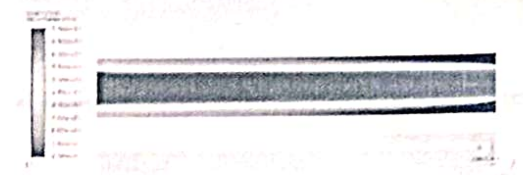Fig. 17 Velocity Contour Results of Twisted Tape Concentric Tube

Fig. 18 Temperature Contour Results of Twisted Tape Concentric Tube

Fig. 19 Temperature Results of Twisted Tape Concentric Tube

The pressure, velocity, and temperature contour results of a simple tape concentric tube heat exchanger is shown in Figures 16, 17, and 18, respectively. The temperature readings at the heat exchanger's intake and exit areas are shown in Figure 19, which offers a thorough summary of the thermal performance. These diagrams can highlight potential areas for improvement and are crucial for understanding the heat transfer process of the exchanger. These temperature profiles may be analysed to find any inefficiencies or places where

changes could be needed to maximize heat transmission. The below table 4 represent the comparative results of the parametric temperature of selected tubes.

Table. 4 Comparative temperature reading

PARAMETER	NORMAL TUBE	PLAIN TAPE	TWISTED TAPE
Inlet Temperature (Hot Fluid)	70	70	70
Outlet Temperature (Hot Fluid)	65.557	65.618	65.068
Inlet Temperature (Cold Fluid)	20	20	20
Outlet Temperature (Cold Fluid)	39.427	39.097	42.237

CONCLUSION

Heat transfer in heat exchangers using plain tubes, plain tape, and twisted tape inserts has been well studied. They came to the conclusion that in turbulent flow, the twisted tape inserts work better. The distribution of temperatures between hot and cold fluids serves as its foundation. The model with the twisted tape insert has the largest temperature distribution, indicating that more heat is transported in this model, according to the temperature data (Table 4). The hot and cold fluids in the twisted tape model saw increases of 22.237 °C and decreases of 4.932 °C, respectively. In terms of heat transmission efficiency, the twisted tape model outperforms the standard and plain tape models by 12% to 16%.

REFFERENCES

[1] Pragneshkumar Prajapati, Umang Soni, Ashvin Suthar (May 2016) "Increase the Heat Transfer Rate of Double Pipe Heat Exchanger with Quadratic Turbulator (Baffle) Attached Twisted Tape Insert" International Journal of Advance Engineering and Research Development Vol. 3, Issue 5, pp. 204-212.

[2] Kanika Joshi, Shivasheesh Kaushik, Vijay Bisht (May 2017) "Investigation on Heat Transfer Rate in Concentric Tube Heat Exchanger Using Pentagonal Shape Inserts in ANSYS FLUENT 14.5 with Varying Mass Flow Rate for Parallel Flow" International Journal of Scientific & Engineering Research, Vol. 8, Issue 5, pp. 1092-1102

[3] Kalapala Lokesh, N Somasankar, Sk Azharuddin, K Uma Maheswara Rao, M Hari Krishna, M Siva Sankar Mani Kumar (May 2017) "Heat Transfer Enhancement of Double Pipe Heat Exchanger Using Twisted Tape Inserts" International Journal of Mechanical Engineering and Technology, Vol. 8, Issue 5, pp. 420-424

[4] Bandu A Mule, D.N.Hatkar, M.S Bembde (August 2017) "Analysis of Double Pipe Heat Exchanger with Helical Fins" International Research Journal of Engineering and Technology, Vol. 04, Issue 08, pp. 961-966

[5] T Vijaya sagar, Dr.Y.Appalanaidu (August 2017) "Experimental Investigation of Heat Transfer Coefficient and Friction Factor in a Double Pipe Heat Exchanger With and Without Twisted Tape Inserts using ZNO-Propylene Glycol Nano Fluid" International Journal of Mechanical Engineering and Technology, Vol. 8, Issue 8, pp. 94-106

[6] J.S. Jayakumar, S.M. Mahajani, J.C. Mandal, P.K. Vijayan, Rohidas Bhoi (October 2017) "Experimental and CFD estimation of heat transfer in helically coiled heat exchangers" Chemical Engineering Research and Design, pp. 222-232.

[7] Yamini Pawar, Ashish Sarode (December 2017) "An Experimentation of Helical Coil Tube Heat Exchanger with Different Curvature Ratio and Geometry" International Conference Proceeding, pp. 176-185.

[8] Deepak Sen, Dr. Alka Agrawal, (January 2018) "Enhancing the Heat Transfer Parameters in Double Pipe Heat Exchanger by Creating Turbulence in Inner and Outer Tube" International Journal for Research in Applied Science & Engineering Technology, Vol. 6, Issue I, pp. 2646-2649.
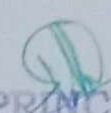
[9] Deepak Kumar S, Saravanan P, Periyannan L (May 2020) "Design And Performance Analysis of Double Pipe Heat Exchanger In Counter Flow", International Journal of Mechanical Engineering, Vol. 7, Issue 5, pp. 8-13.

[10] Folaranmi Joshua (Oct 2009) "Design and Construction of a Concentric Tube Heat Exchanger", AU J.T, Vol. 13, Issue 2, pp. 128-

[11] Karthik Silaipillayarputhur, Tawfiq Al Mughanam, Abdulaziz Al Mojil and Mohammed Al Dhmoush (2017), "Analytical and Numerical Design Analysis of Concentric Tube Heat Exchangers – A Review", Materials Science and Engineering.

[12] Pitchandi K (2014), "Design and analysis of concentric tube heat exchanger using entropy generation minimisation", Int. J. Exergy, Vol. 15, Issue 03, pp. 276-295.

PRINCIPAL
Ganesh College of Engineering
Attur Main Road, Mettupatti
SALEM-636 111